

# ON PITCH-ANGLE SCATTERING RATES OF INTERSTELLAR PICKUP IONS AS DETERMINED BY IN SITU MEASUREMENT OF VELOCITY DISTRIBUTIONS

LUKAS SAUL,<sup>1,2</sup> EBERHARD MÖBIUS,<sup>1</sup> PHILIP ISENBERG,<sup>1</sup> AND PETER BOCHSLER<sup>2</sup>

Received 2006 May 8; accepted 2006 September 20

## ABSTRACT

Newly ionized interstellar atoms are acted upon by electromagnetic forces in the solar wind. Measurements of these pickup ions enable study of the transport processes controlling the evolution of charged particle populations in solar wind plasma. Data from the CELIAS instruments on board the *SOHO* spacecraft allow measurement of the velocity distribution of singly charged helium ions. These observations are compared to the predictions of a hemispheric model of pitch-angle diffusion. To justify the use of the hemispheric model we show here that a “resonance gap,” which hinders cross-hemispheric scattering of protons by Alfvén waves, can exist for the case of pickup helium scattered by outward-propagating waves. We find that the observed shape of helium pickup ion velocity distributions is consistent with the hemispheric model prediction. The parallel mean free path is found to vary with wave power from values of 0.1 to over 1 AU, here presented as a first measurement of the parallel mean free path as a function of magnetic wave power. Magnetic field data from the *Wind* spacecraft enable comparison to the coincident magnetic field wave power. The cross-hemispheric scattering rate is found to be monotonic and exponentially dependent on wave power over the dynamic range considered.

*Subject heading:* solar wind

## 1. PICKUP ION TRANSPORT IN THE SOLAR WIND

The Sun resides in a diffuse medium of gas and dust. As neutral atoms from this gas approach the Sun, they become susceptible to ionization processes. Once ionized, they become a component of the magnetized solar wind plasma and are subject to electromagnetic forces in the interplanetary medium.

Although the subsequent evolution of the pickup ion (PUI) distribution is described completely by the Vlasov equation, we cannot apply it in full detail as we are not privy to knowledge of the electric and magnetic fields everywhere in the interplanetary medium. In particular, fluctuations of the interplanetary magnetic field (IMF) such as Alfvén waves can interact with the PUI distribution, causing pitch-angle scattering and other transport effects. Due to the random nature of these fluctuations, they can be described by a diffusive approximation. This is the quasi-linear approach to modeling the evolution of charged particle distributions, including cosmic rays and solar energetic particles (e.g., Jokipii 1974; Fisk et al. 1974). Here we consider the PUI population as a probe of the dependencies of pitch-angle scattering rates on such fluctuations.

### 1.1. Pickup Ion Pitch-Angle Diffusion

When the PUIs are injected into the solar wind they are highly anisotropic, forming a ring distribution in velocity space (see Fig. 1). Magnetic field fluctuations such as Alfvén waves in the solar wind are usually assumed to isotropize the distribution quickly (e.g., Vasylunas & Siscoe 1976), effectively smearing the ring onto a spherical shell. In this interaction the PUIs do not gain or lose energy (in the solar wind frame), but are merely deflected in direction by the Lorentz force.

However, observations have shown that PUIs are not immediately isotropized in pitch angle and may have parallel mean free paths in the inner heliosphere as large as 1 AU (Gloeckler et al. 1995; Möbius et al. 1998; Oka et al. 2002). The pitch-angle scattering rate has been observed to be correlated with IMF wave

power (Saul et al. 2004), as expected from quasi-linear theory. Here we further explore the relation between pitch-angle scattering rates and IMF wave power, comparing the velocity distribution to the prediction of an ion transport model, allowing an explicit measurement of the cross-hemispheric pitch-angle scattering rate and its dependence on magnetic wave power.

## 2. INSTRUMENTATION

The CTOF sensor, in the CELIAS package on board *SOHO*, is well suited to study the variability of helium pickup ions. Its location at the L1 point and its relatively large geometric factor allow the best time resolution of the He<sup>+</sup> velocity distribution currently available (Hovestadt et al. 1995). The energy and angular acceptance of the instrument, for which identification of pickup ions is clear, is shown in Figure 1 on the spherical volume of the PUI distribution in velocity space. The aperture points sunward and therefore detects only antisunward moving particles, and does not give further angular information about the incoming particles. Despite this lack of angular information, the velocity distribution during times of different IMF orientation can be used to determine pitch-angle scattering rates.

Although *SOHO* was not equipped with a magnetometer, the relatively close location of the *Wind* spacecraft has been used to estimate the magnetic field conditions at *SOHO*. Magnetic field parameters are calculated at the location of *Wind* (Lepping et al. 1995) and then convected to the position of *SOHO* assuming a frozen in field. This shift of the *Wind* data is performed using the orientation of the IMF from *Wind* and the solar wind speed as measured by the proton monitor of CELIAS on *SOHO* (Ipavich et al. 1998). For the IMF parameters considered herein (orientation, magnitude, and fluctuation wave power), the separation distance between the spacecraft is quite small compared to correlation lengths, suggesting that the convection technique allows a relatively accurate determination of these parameters (see also Matsui et al. 2002, as used in Saul et al. 2004).

## 3. THE HEMISPHERIC MODEL

In order to interpret the velocity distribution of pickup helium, we must consider a model of the transport and diffusion in pitch

<sup>1</sup> University of New Hampshire, Durham, NH.

<sup>2</sup> University of Bern, Switzerland.

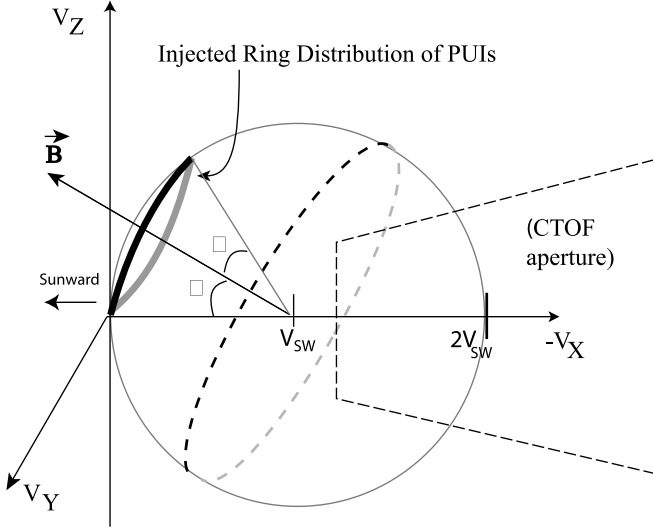


FIG. 1.—Diagram showing a newly injected pickup ion distribution in velocity space (spacecraft frame), in an oblique IMF. The portion of PUI velocity space sampled by the energy range of *SOHO* CTOF is shown as a dashed quadrilateral. The dashed circle on the sphere indicates  $\mu = 0$ .

angle that the distribution undergoes as it is carried outward in the solar wind. Observations show that the Vasyliunas & Siscoe (1976) model of instantaneous pitch-angle scattering is not exact, and so we must consider a finite pitch-angle diffusion coefficient.

The Fokker-Planck pitch-angle diffusion coefficient is in general a function of pitch angle, and for the case of resonant wave–proton interactions with parallel-propagating waves, this coefficient tends toward zero for pitch angle  $\alpha = 90^\circ$ , or  $\mu = \cos \alpha = 0$  (e.g., Jokipii 1974). The precise dependence of pitch-angle scattering rates on the magnetic field fluctuation spectrum has been the subject of much theoretical work, mostly in terms of the application of quasi-linear theory (see also, e.g., Hasselmann & Wibberenz 1970; Schlickeiser 1998; Lu & Zank 2001).

With this motivation we consider here an anisotropic model of pitch-angle scattering, in which pickup ions are expected to scatter quickly in either hemisphere of velocity space but scatter slowly by diffusion across  $90^\circ$  pitch angle, following Isenberg (1997). Particles are effectively scattered when their gyrofrequencies are in resonance with the fluctuating field, i.e., when the Doppler-shifted frequency of the fluctuation as observed by the moving particle is equal to an integer multiple of the gyrofrequency. This can be expressed in the lowest order resonance condition, written here for the case of helium:

$$\omega - k_{\parallel} v_{\parallel} = -\Omega_{\text{He}}. \quad (1)$$

Here  $\omega$  and  $k_{\parallel}$  are the wave frequency and component of the wavevector parallel to the magnetic field, and  $\Omega_{\text{He}}$  is the gyrofrequency of helium. If diffusion across  $90^\circ$  pitch angle is suppressed due to a lack of the required resonant waves as the parallel velocity goes to zero, this is referred to as a “resonance gap.” Particles are then only scattered through this barrier by changes in mean field or nonresonant interactions.

### 3.1. Resonance Gap for Helium

The character of the resonance gap at  $\mu = 0$  depends on the nature of the waves doing the scattering as well as the species being scattered. A resonance gap can exist for cases other than protons scattered by pure Alfvén waves, including scattering by bidirectional wave propagation and some kinds of turbulence

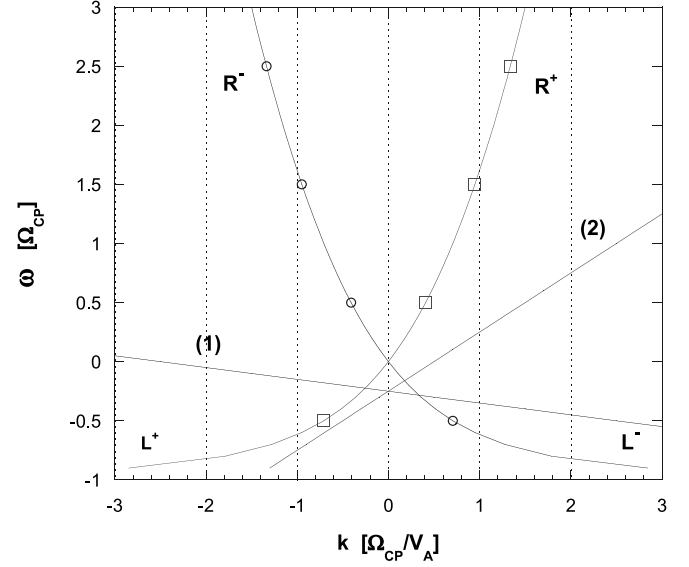


FIG. 2.—Dispersion relations for parallel-propagating Alfvén waves are shown with two examples of the resonance condition for helium. The wave polarization and direction is indicated in each quadrant, and outgoing (incoming) waves are marked with squares (circles). The frequency is expressed in terms of the proton gyrofrequency, and the wavenumber in terms of the gyrofrequency over the Alfvén speed. Line 1 corresponds to  $v_{\parallel} = -0.1 V_A$ , which exhibits resonance with both incoming and outgoing waves, while line 2 corresponds to  $v_{\parallel} = 0.5 V_A$  and has no resonance with outgoing waves.

(e.g., Ng & Reames 1995; Isenberg et al. 2003). In particular, the case for a hemispheric structure is not as clear for pickup helium as for protons, and so we justify the hemispheric approach for this species here.

The details of this interaction depend on the dispersion relation of the waves in question, the location of the wave power in  $\omega$  and  $k$  space, and the location at which the dispersion relation intersects the helium resonance condition:  $\omega - k_{\parallel} v_{\parallel} = -\Omega_{\text{He}}$ . If we consider only parallel-propagating Alfvén waves at frequencies near the proton gyrofrequency, the dispersion relation can be written as

$$\omega_{\pm}^2(k) = k_{\pm}^2 V_A^2 \left( 1 + \frac{\omega_{\pm}}{\Omega_{\text{CP}}} \right), \quad (2)$$

where  $V_A$  is the Alfvén speed,  $\Omega_{\text{CP}}$  is the proton cyclotron frequency, and the  $\pm$  indicates outgoing (+) or incoming (−) waves.

The intersections of the graphs of the dispersion relation (2) with the resonance condition (1) can be seen in Figure 2 for two different parallel velocities. Positive and negative frequencies here indicate the polarization state (R or L). The intersections represent locations in  $\omega$  and  $k$  space for which resonant pitch-angle scattering can occur (Dusenbury & Hollweg 1981). From Figure 2 it can be seen that parallel velocities (or pitch angles) exist for which there is no resonance with purely ingoing or outgoing Alfvén waves.

The resonant frequency for a given parallel velocity can be found by combining equations (1) and (2) to eliminate the wavevector, and by considering only outward-propagating waves (i.e., assuming a dominant sunward source of waves in the inner heliosphere). Simplifying the expression yields

$$\frac{v_{\parallel}(\omega)}{V_A} = \left( 1 + \frac{\Omega_{\text{CP}}}{4\omega} \right) \sqrt{1 + \frac{\omega}{\Omega_{\text{CP}}}}. \quad (3)$$

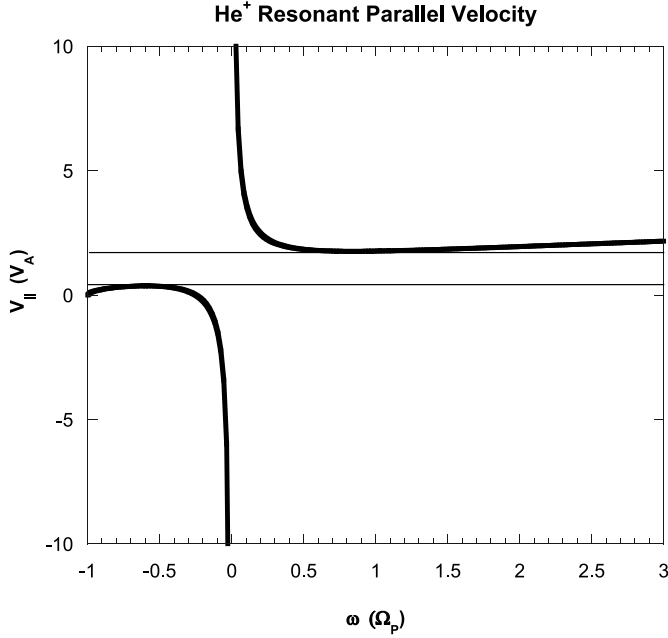


FIG. 3.— Parallel velocity of a helium PUI in resonance with outgoing Alfvén waves (in units of the Alfvén speed) vs. the wave frequency (in units of the proton cyclotron frequency) (eq. [3]). The resonance gap, or range of parallel velocities not at resonance with any frequency, is shown between horizontal lines.

Here the factor of 4 comes from the mass ratio of the  $\text{He}^+$  to  $\text{H}^+$ . This resonant parallel velocity is shown graphically in Figure 3, with the range of helium parallel velocities not resonant with outgoing waves indicated, duplicating the procedure used by Dusenbury & Hollweg (1981) for the case of  $\text{He}^+$ . The boundaries of the indicated resonance gap can be solved by setting the derivatives of equation (3) with respect to the frequency equal to zero. They are given by

$$\frac{v_{||,\text{critical}}}{V_A} = \left( \frac{15 \mp \sqrt{33}}{16} \right) \left( \frac{-3 \pm \sqrt{33}}{1 \pm \sqrt{33}} \right)^{1/2} = \left\{ \begin{array}{l} 0.36 \\ 1.76 \end{array} \right\}, \quad (4)$$

where the parallel velocities are expressed in terms of the Alfvén speed. The solar wind is highly super-Alfvénic, and so these critical parallel velocities are quite small compared to the velocity of a pickup ion, corresponding to pitch angles near  $90^\circ$ . For this reason, we can approximate this resonance gap for helium to exist at  $v_{||} = 0$  or  $\mu = 0$ .

### 3.2. The Hemispheric Model with Helium

In his model, Isenberg (1997) treats the full transport equation analytically, assuming the pitch-angle diffusion coefficient is an inverse delta function in pitch-angle space, being infinite everywhere except at  $\mu = 0$ , where it is finite. This effectively reduces the problem to a first-order anisotropic treatment, dividing the PUI distribution function into two hemispheres in velocity space, where fast scattering leads to isotropy in each hemisphere (see Fig. 4). The model is modified when appropriate for our consideration of singly charged interstellar helium PUIs, assuming that a decrease in scattering rate occurs near  $\mu = 0$ . Remarkably, an analytic solution exists for the case of radial magnetic field, and for the assumption that the pitch-angle scattering rate at  $90^\circ$  scales as  $K_{\mu=0} \sim v/r$ , the velocity of a particle divided by its heliocentric distance. This solution can be expressed as an integral of Bessel functions. The velocity distribution in the anti-

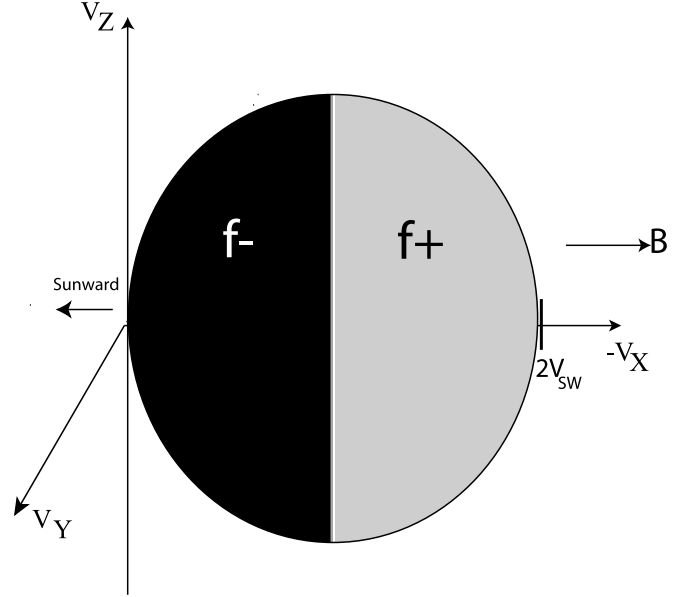


FIG. 4.— Diagram showing a hemispheric pickup ion velocity distribution in radial field (spacecraft frame). The distribution is characterized by the two phase-space densities  $f_-$  and  $f_+$ , while scattering between the hemispheres is characterized by the dimensionless diffusion coefficient  $D$ . Pickup ions begin in the  $f_-$  or sunward portion of the distribution.

sunward hemisphere takes the form, given by equation (9) of Isenberg (1997),

$$f(w, r) = \frac{3\beta_0 r_0^2}{8\pi V_{\text{SW}}^4} \frac{D+1}{r w^{3/2}} \exp(-aD) \times \int_0^{2a} N[r w^{3/2} \exp(z-a)] J_0(\Phi) dz. \quad (5)$$

Here  $\beta_0$  is the ionization rate at a distance  $r_0$ ,  $w$  is the normalized velocity  $v/V_{\text{SW}}$ ,  $r$  is the heliocentric distance,  $a = 3(1-w)/4$ , and the argument of the Bessel function  $J_0$  is  $\Phi = [z(2a-z)(1-D^2)]^{1/2}$ ;  $D$  is a dimensionless scattering parameter representing the cross-hemispheric diffusion rate, defined as  $D = K_{\mu=0} 2r/v$ . The inflowing neutral particle density  $N(r)$  considered in Isenberg (1997) was that of hydrogen, for which the radiation pressure nearly balances the gravitational force. We use here a different model for the neutral helium density.

To calculate the neutral density we consider cold interstellar neutrals on the upwind side of the heliosphere, which is justified by the upwind locations of *SOHO* during the period of observation and the small difference between cold and the hot models here. This allows us to solve for a steady state density of neutral helium as a function of heliocentric distance:

$$N(r) = A \exp \left( -\frac{\beta_0 r_0^2}{GM_\odot} \sqrt{v_\infty^2 + \frac{2GM_\odot}{r}} \right). \quad (6)$$

Here we have used the fact that radiation pressure does not influence the trajectory of the incoming noble gas atoms, and we take the ionization rate at 1 AU as  $\beta_0 = 3.0 \times 10^{-8} \text{ s}^{-1}$  (Rucinski et al. 1996) and the motion of a neutral atom far from the Sun as  $v_\infty = 26.3 \text{ km s}^{-1}$  (Möbius et al. 1995). The normalization factor  $A$  is chosen so that the interstellar density is recovered for large  $r$ .

It is important to note that this model includes not only the effects of pitch-angle scattering between the two hemispheres,

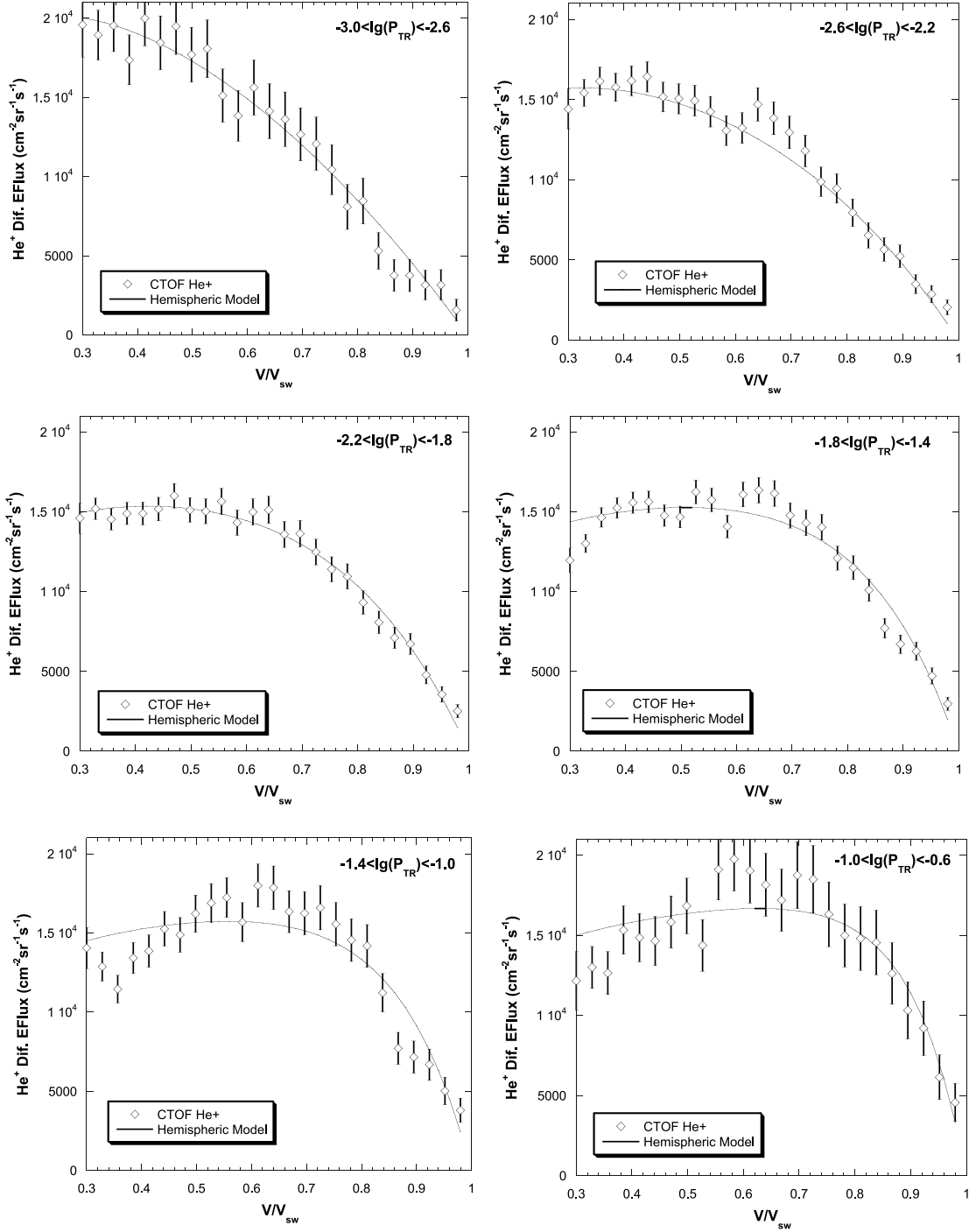


FIG. 5.— *SOHO* CTOF helium energy flux velocity spectra averaged over times of indicated transverse wave power in near-radial IMF, in the solar wind frame. The best-fit hemispheric model is shown as a continuous line. The associated best-fit parameter for each plot is given in Fig. 6.

but also convection terms including adiabatic focusing due to the diverging magnetic field. As pointed out by Isenberg (1997), this focusing acts to bring some particles from one hemisphere to the other even in the absence of pitch-angle scattering. Although this solution (eq. [5]) is only strictly valid in the case of radial magnetic fields, we compare here data taken with the IMF of less than  $15^\circ$  from the radial direction.

#### 4. PROCEDURE AND RESULTS

We wish to compare the model of the pickup ion velocity distribution described above to in situ measurements of singly charged helium. To do so requires that the individual  $\text{He}^+$  detections be

added to a velocity histogram in the normalized velocity  $v/V_{\text{sw}}$ . An individual helium event, which corresponds to a range of velocities due to the finite energy passband of the instrument, is translated to a range in  $v/V_{\text{sw}}$  using the CELIAS proton monitor data from the same time period.

The energy flux density is tabulated in a histogram, by multiplying the calibrated number fluxes  $J_i$  from the count rates by the midpoint energy in the associated  $i$ th energy bin. The energy flux density is used here because this quantity is predicted to be independent of the solar wind speed, in contrast with the phase-space density or number flux (Vasyliunas & Siscoe 1976; Möbius et al. 1995).

#### 4.1. Calculation of Resonant Wave Power

A superposed epoch analysis is used to include all helium events from solar wind with specific IMF wave powers. The resonant transverse wave power is calculated from 3 s IMF vector measurements by *Wind* MFI. We use Fourier analysis in mean field coordinates to determine components of the power spectrum distribution of IMF variations. The frequency range considered is from 0.002 to 0.16 Hz (the Nyquist frequency for the 3 s public MFI data). It is not possible to uniquely identify frequency and wavevectors with only a single spacecraft, so this range of frequencies is used as an indicator of resonant wave power. The typical  $\text{He}^+$  gyrofrequency in the solar wind is 0.015 Hz ( $2nT$ ) to 0.15 Hz ( $20nT$ ).

The power spectrum is computed for each contiguous 15 minute period in the data set, and each component fit to a power law with the least-squares method. A sliding principal axis coordinate system was used to determine each power spectrum distribution. The principal axes for each 3 s field vector were calculated using a 15 minute sliding mean field direction  $\hat{\mathbf{B}}$ . The  $z$ -component is chosen along the mean field,  $x$  along  $\hat{\mathbf{B}} \times \mathbf{r}$ , and  $y$  along  $\hat{\mathbf{B}} \times (\hat{\mathbf{B}} \times \mathbf{r})$ . We consider here the transverse power  $P_{\text{TR}}$ , the power in all perpendicular (or transverse) fluctuations (see, e.g., Matthaeus & Smith 1981). The quantity  $P_{\text{TR}}$  is taken from the power-law fit and is thus affected by wave power over the entire frequency range considered. The numerical value used to sort the helium events is the value of the power-law fit of the spectral component  $P_{\text{TR}}$  evaluated at 0.1 Hz.

#### 4.2. Model Fit Procedures

The model discussed in § 3 was compared to the PUI data from CELIAS taken during times of near-radial IMF ( $0^\circ$  to  $15^\circ$ ), and for several different ranges of the resonant wave power as described above. Before the data were compared to the model, the spectra combined in the analysis were shifted in velocity space according to the day of year, to compensate for the shift of the distribution due to the change in the injection velocity over the year (see Möbius et al. 1999). This is necessary as the model used here assumes a zero injection velocity for the pickup ions in the heliocentric frame. Finally, helium counts at higher speeds than the nominal cutoff at twice the solar wind speed were ignored as the model used does not include energy diffusion or acceleration processes. This suprathermal flux is nominally at least an order of magnitude less than the bulk PUI flux.

To compare the observation with the model, a two-parameter least-squares fitting procedure was used, implementing the simplex method for minimization. The free parameters in the model (eq. [5]) are the scattering rate  $D$  and an arbitrary normalization factor (not affecting the shape of the velocity spectrum).

The predicted distribution function is a function of pitch angle, and to predict the measured flux this must be integrated over the aperture of the instrument according to the entrance system calibration (Aellig & Bochsler 1998). The hemispheric model predicts no angular dependence of the distribution function over the instrument aperture, as the aperture is entirely in the antisunward hemisphere in velocity space. Therefore no such integration is required for this study, although a numerical integration is required in computing equation (5).

#### 4.3. Best-Fit Parameters

Results of the data and model fits are shown in Figure 5, where the data and best-fit models are shown for six ranges of transverse wave power. The data in these spectra are from March to September of 1996, including all time periods in which the magnetic

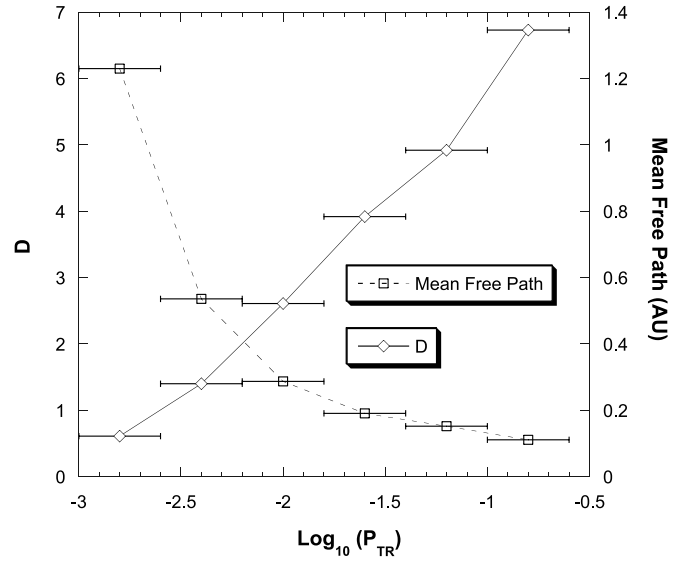


FIG. 6.— Best-fit dimensionless hemispheric diffusion coefficient  $D$  vs. log of the transverse wave power, on the left-hand  $y$ -axis scale. The associated parallel mean free path is also shown, on the right-hand  $y$ -axis scale. The dependence of diffusion rate on wave power can be seen to be monotonic and approximately exponential.

wave power was as indicated and the mean field was near radial. The difference between the helium spectra taken during different levels of IMF wave power can be seen most prominently in the steepness of the cutoff. For faster pitch-angle scattering rates, the cutoff becomes steeper as more recently ionized helium that has not been cooled enters the antisunward hemisphere and can be sampled by the instrument. Some change in the shape of the distribution can also be seen at lower PUI velocities. It is evident from Figure 5 that the shape of the PUI distribution is well predicted by the hemispheric model. Our attempts to fit the velocity distribution with a diffusion model including a constant diffusion coefficient (independent of pitch angle), and assuming instantaneous diffusion, were not as successful in fitting the observations (not shown).

The best-fit parameters to the hemispheric model are shown in Figure 6. The dimensionless scattering rate parameter  $D$  is shown as a function of the wave power. A clear monotonic trend is present, confirming our hypothesis that more IMF wave power leads to more pitch-angle isotropization (e.g., Saul et al. 2004).

For each velocity distribution we calculated the associated parallel mean free path for each model and range of wave power, as shown on the right-hand  $y$ -axis in Figure 6. The parallel mean free path in this case is defined as (e.g., Hasselmann & Wibberenz 1970; Isenberg 1997)

$$\lambda_{\parallel}(v) = \frac{3v}{8} \int_{-1}^1 \frac{1 - \mu^2}{D_{\mu\mu}} d\mu, \quad (7)$$

where the denominator of the integrand is inversely proportional to delta function in pitch angle for the hemispheric model. For the hemispheric model, this results in

$$\lambda_{\parallel} = \frac{3r}{4D}. \quad (8)$$

For the calculation of an associated mean free path in Figure 6 we used a heliocentric distance  $r = 1$  AU.

## 5. DISCUSSION OF RESULTS

In summary, we have found the following:

1. A hemispheric model of pitch-angle anisotropy predicts the observed spectrum of interstellar pickup helium remarkably well.
2. Pitch-angle scattering rates of interstellar pickup helium ions as calculated from the hemispheric model were found to increase monotonically and nearly exponentially in transverse wave power.
3. The parallel mean free path was found to vary between 0.1 and 1.2 AU over the range of dynamic wave power considered.
4. A resonance gap can exist for helium, in the case of scattering by outward-propagating Alfvén waves.

The observed monotonic trend of pitch-angle scattering rate with increasing transverse resonant wave power supports the standard picture of resonant pitch-angle scattering. However, the pitch-angle scattering rates were found to be exponential with transverse resonant wave power. The predicted isotropic pitch-angle diffusion coefficient from quasi-linear theory is linear in the wave power (e.g., Fisk 1974), compared with the exponential dependency observed here in applying the hemispheric model (see Fig. 6). The reason for this increased dependency on wave power is unclear at this time, but probably results from the controlling effect of the scattering across the resonance gap. A model of this cross-hemispheric scattering rate will need to rely on non-resonant scattering or less dominant wave modes.

The large parallel mean free path derived from the observations is not unreasonable. Observed PUI anisotropies (Gloeckler et al. 1995; Möbius et al. 1998; Oka et al. 2002) suggest pitch-angle scattering mean free paths on the order of an astronomical unit. This analysis based on the hemispheric model shows parallel mean free paths that do not average below 1/10 of an AU even at the highest wave powers. We also find mean free paths as large as 1.2 AU for the case of the lowest wave power considered.

These results are derived from data taken during solar minimum, in the ecliptic. Pitch-angle scattering rates could differ during more active time periods, or different latitudes. The pitch-angle scattering rates derived here are also very much model-dependent, as they are derived from fitting the hemispheric model to measured velocity distributions. Potential variations from the assumptions in the model are possible. While we have used velocity distributions here to determine pitch-angle anisotropies, a direct measurement of the instantaneous pitch-angle distribution via angular discrimination of particle events would enable a more accurate comparison to the model. This may become possible with the next generation of space plasma instrumentation, such as the PLASTIC instrument to be launched with the *STEREO* mission. Finally, comparison of the observed distributions to other models, such as those of Lu & Zank (2001), could also yield different values for the pitch-angle scattering rates.

This material is based on work supported by the National Science Foundation under grant 0502324. Any opinions, findings, and conclusions or recommendations expressed in this material are those of the authors and do not necessarily reflect the views of the National Science Foundation. Chuck Smith and Marty Lee also contributed to understanding and motivating this research. This work was also partially supported by NASA grants NAG5-10890, NAG5-12929, NNG06GD55G, and NNG04GA24G. The Swiss National Foundation and the *SOHO* and *Wind* teams are also acknowledged, as are the hospitality of the University of New Hampshire Department of Physics and the Institute for the Study of Earth, Oceans, and Space, and the hospitality of the Space Research and Planetary Sciences Department of the University of Bern.

## REFERENCES

- Aellig, M. R., & Bochsler, P. 1998, Ph.D. thesis, Univ. Bern  
 Dusenbury, P. B., & Hollweg, J. V. 1981, *J. Geophys. Res.*, 86, 153  
 Fisk, L. A., Goldstein, M. L., Klimas, A. J., & Sandri, G. 1974, *ApJ*, 190, 417  
 Gloeckler, G., Schwadron, N. A., Fisk, L. A., & Geiss, J. 1995, *Geophys. Res. Lett.*, 22, 2665  
 Hasselmann, K., & Wibberenz, G. 1970, *ApJ*, 162, 1049  
 Hovestadt, D., et al. 1995, *Sol. Phys.*, 162, 441  
 Ipavich, F. M., et al. 1998, *J. Geophys. Res.*, 103, 17205  
 Isenberg, P. A. 1997, *J. Geophys. Res.*, 102, 4719  
 Isenberg, P. A., Smith, C. W., & Matthaeus, W. H. 2003, *ApJ*, 592, 564  
 Jokipii, J. R. 1974, *ApJ*, 194, 465  
 Lepping, R. P., et al. 1995, *Space Sci. Rev.*, 71, 207  
 Lu, J. Y., & Zank, G. P. 2001, *ApJ*, 550, 34  
 Matsui, H., Farrugia, C. J., & Torbert, R. B. 2002, *J. Geophys. Res.*, 107, 1355  
 Matthaeus, W. H., & Smith, C. 1981, *Phys. Rev. A*, 24, 2135  
 Möbius, E., Rucinski, D., Hovestadt, D., & Klecker, B. 1995, *A&A*, 304, 505  
 Möbius, E., Rucinski, D., Lee, M. A., & Isenberg, P. A. 1998, *J. Geophys. Res.*, 103, 257  
 Möbius, E., et al. 1999, *Geophys. Res. Lett.*, 26, 3181  
 Ng, C. K., & Reames, D. V. 1995, *ApJ*, 453, 890  
 Oka, M., Terasawa, T., Noda, H., Saito, Y., & Mukai, T. 2002, *Geophys. Res. Lett.*, 29, 54  
 Rucinski, D., et al. 1996, *Space Sci. Rev.*, 78, 73  
 Saul, L., Möbius, E., Smith, C. W., Bochsler, P., Grünwaldt, H., Klecker, B., & Ipavich, F. M. 2004, *Geophys. Res. Lett.*, 31, L05811  
 Schlickeiser, R. 1998, *ApJ*, 492, 352  
 Vasyliunas, V. M., & Siscoe, G. L. 1976, *J. Geophys. Res.*, 81, 1247